

# Mechanism of Hydroxyapatite/Chitosan Composite Precipitation From Aqueous Solution at Room Temperature and Alkali Environment

F. Abida, A. Elouahli, A. Bourouisse, M. Jamil, ELH. Gourri, M. Ezzahmouly, Z. Hatim  
Team of Electrochemistry and Biomaterials, Department of Chemistry, Faculty of Sciences,  
University of Chouaib Doukkali, El Jadida, Morocco.

**Abstract**— The process of hydroxyapatite/chitosan precipitation from aqueous solution, at room temperature and alkali environment, was examined by chemical analysis, Infrared Spectroscopy and X-ray diffraction. The results show, in the presence as in the absence of the chitosan, initially the fast formation of amorphous octocalcium phosphate ( $\text{Ca}_8(\text{HPO}_4)_2(\text{PO}_4)_4 \cdot n\text{H}_2\text{O}$ : OCPam) and fast transferring from OCPam to apatitic-tricalcium phosphate: ( $\text{Ca}_9(\text{HPO}_4)(\text{PO}_4)_5(\text{OH})$ : TCPap), then from TCPap to calcium-deficient hydroxyapatite ( $\text{Ca}_{10-x}(\text{HPO}_4)_x(\text{PO}_4)_{6-x}(\text{OH})_{2-x}$ : ACP) and to stoichiometric hydroxyapatite ( $\text{Ca}_{10}(\text{PO}_4)_6(\text{OH})_2$ : HAP). The transformation TCPap-ACP was slightly inhibited in the presence of chitosan. A stable ACP-chitosan complex was formed, and then evolved into Hydroxyapatite / chitosan composite. The materials can have potential medical applications such as bone regenerating scaffold.

**Index Terms**— Biomaterials, composite materials, precipitation, phase transitions.

## 1 INTRODUCTION

**S**YNTHETIC calcium-hydroxyapatite ( $\text{Ca}_{10}(\text{PO}_4)_6(\text{OH})_2$ : HAP) has been used extensively for biomedical implant applications and bone regeneration due to its bioactive and osteoconductive properties [1],[2]. In recent years, HAP-reinforced degradable polymers have been developed to fix bone fractures [3],[5]. Polymers of natural origin such collagen; gelatin, alginate, chitosan and cellulose are attractive options, mainly due to their similarities with extracellular matrix (ECM) as well as chemical versatility and biological performance. When the polymer matrix is reabsorbed, new bone may intergrow around the HAP particles. Due to its ability to promote proliferation and mineral deposition by osteoblasts, chitosan has been extensively used for bone tissue engineering [6],[8]. In particular, because the bone ECM is composed of organic and inorganic phase composite materials of chitosan and HAP, it could be used as implants in orthopedic surgery for a scaffold base for medical applications [9],[10],[11],[12].

As a linear polysaccharide, chitosan is a partially deacetylated derivative of chitin. (an important constituent of the exoskeleton in animals) and is the second most abundant biosynthesized material.

• Corresponding author: M. Jamil  
E-mail: mo.jamil@yahoo.fr

Structurally, it is composed of B (1-4)-linked D-glucosamine residues with a variable number of randomly located N-acetyl-glucosamine groups. The ratio of glucosamine to the

sum of glucosamine and N-acetyl-glucosamine is defined as the degree of deacetylation (DD). The average molecular weight (Mw) of chitosan can range from 300–1,000 kDa with a DD of 30–95%, depending on the source and preparation procedure. Mw and DD are the predominant parameters that influence the solubility, mechanical strength, and degradation properties of chitosan and chitosan-based biomaterials [13],[14].

Several new forms of biocomposite HAP/chitosan in form of hydrogel, films, sponges and granules have been developed and different preparation methods have been reported, such as the mixing of HAP powder in chitosan solution and the coating of HAP particles onto a chitosan sheet [15],[16]. However, the composites obtained in some cases were not homogeneous and can cause inflammation when implanted. Composites with a homogeneous mixture have been prepared from cement method, via In-Situ Hydration or by a coprecipitation method [10],[17],[18],[19].

The most previous studies generally focus on the preparation methods and on the microstructure of biocomposites but the mechanism and kinetics of HAP/chitosan formation are still misunderstood.

The aim of this study is to investigate the process of coprecipitation of hydroxyapatite/chitosan composite. The synthesis was carried out by reaction between  $\text{H}_3\text{PO}_4$ /chitosan solution and  $\text{Ca}(\text{NO}_3)_2 \cdot 4\text{H}_2\text{O}$  solution at 25°C in alkali environment.

## 2 MATERIALS AND METHODS

### 2.1 Preparation of chitosan powder

Chitin was extracted from carapaces of prawns, washed, crushed and then demineralized using repeated baths of diluted chloride acid (0,2N) and deproteinized by repeated baths of aqueous solution of sodium hydroxide (0,5N). Chitin product was treated with 45wt% aqueous sodium hydroxide at 100°C for 8 h to give chitosan. The obtained flakes were then purified by solubilization in the presence of acetic acid (1wt %) and precipitation at pH=8 in the presence of NaOH (1N) and intensive washings with deionized water/glycerol solution. The obtained powder of chitosan was dried at 45°C and preserved at 5°C until its use.

### 2.2 Preparation of bio-composite hydroxyapatite / chitosan

The purified chitosan was solubilized in acetic acid solution (1wt %). After stirring, the chitosan aqueous solution of 2wt % was filtered then added to the orthophosphoric acid solution (1M). The obtained solution was well mixed by stirring. The orthophosphoric acid / chitosan ratio was adjusted to the final composition of the bio-composite HAP/Chitosan (100/00, 80/20, 75/25 and 70/30%, percentages in mass). The orthophosphoric/chitosan acid solution was added to the calcium nitrate solution (0,5M) at 25°C and under stirring. The atomic rapport Ca/P was adjusted to 1,667 (ratio of the stoichiometric hydroxyapatite). The pH of the mixture was maintained to 10 with ammonium hydroxide. Once the addition of the acid mixture was completed, maturation continued for the determined times in a closed balloon. The result obtained after maturation was filtered then stored in the freezer at -5°.

### 2.3 Characterization

The mass fraction of calcium and phosphore were carried out, at different reaction times, by inductively coupled plasma mass spectroscopy (ICP-AES) (ThermoJarrel Ash. Atom Scan 16). We used the wavelength characteristic of calcium  $\lambda = 317,933\text{nm}$  and of phosphore  $\lambda = 213,618\text{nm}$ . The mass fraction of ions traces were also carried out by ICP-AES. The precipitates sample was characterized by Infrared Spectroscopy FTIR (KBr pellet method, Bio-Rad Win-IR Pro). Diffractometer Siemens D5000 was employed to identify precipitates phases and diffractometer (SEIFERT XRD 3000) was used for an acquisition of data to the small angles. The degree of deacetylation (DD) of the chitosan was calculated from <sup>1</sup>HMRN and the average molecular weight was determined by viscometer.

## 3 RESULTS AND DISCUSSION

### 3.1 Chitosan

The purity of the chitosan was confirmed by chemical analysis. The presence of ion traces like Mg, Zn and Ca can

have an influence on the kinetics of formation of the hydroxyapatite [20],[21]. 18 ions' traces have been analysed. These ions are present with concentration less than 0,05wt %.

The degree of deacetylation (DD) of chitosan was found to be close to  $83 \pm 2\%$ , and the average molecular weight was 500.000.

Figure 1(a) shows the FTIR spectra of chitosan. The absorption bands observed around 2883, 1661, 1604, 1551 $\text{cm}^{-1}$  were assigned to methylene (-CH<sub>2</sub>), amide I (C=O), amino (-NH<sub>2</sub>) and amide II (-NH), respectively. The band around 3420  $\text{cm}^{-1}$  was assigned to water and to the primary amine functional group; the bands around 2054  $\text{cm}^{-1}$  were attributed to elongations of the CO<sub>2</sub> functional group, while the band around 1096  $\text{cm}^{-1}$  corresponded to C-O-C elongation.

Figure 1(b) shows X-ray diffraction patterns of chitosan, the peak found around  $2\theta=20^\circ$ , was assigned to chitosan chains, aligned through intermolecular interactions.

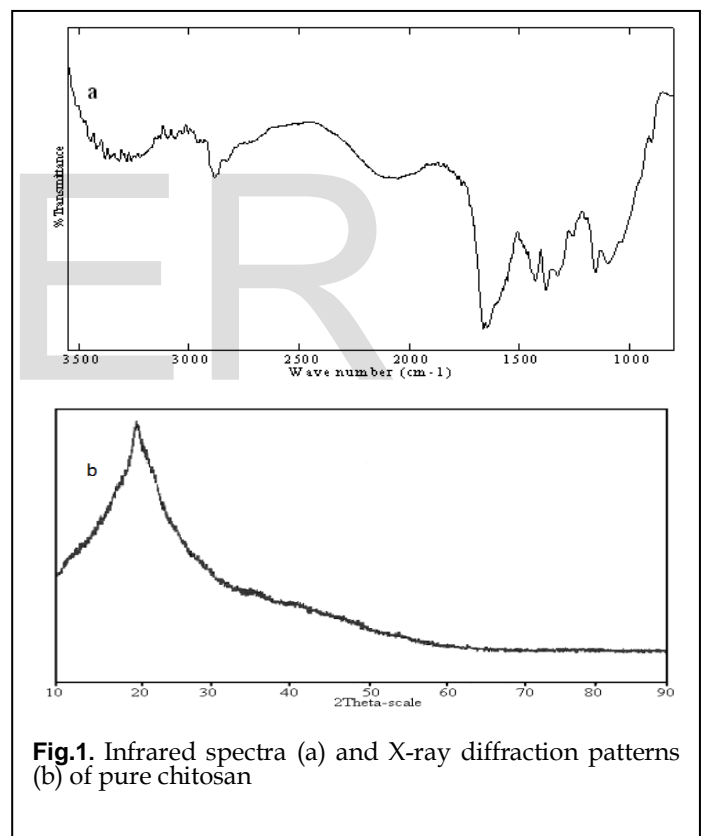


**Fig.1.** Infrared spectra (a) and X-ray diffraction patterns (b) of pure chitosan

### 3.2 Bio-composite hydroxyapatite / chitosan

Strong agglomeration was observed for two slurry bio-composites HAP/Chitosan: 75/25 and 70/30%. In this paper

we present the results concerning the sample HAP/Chitosan: 100/00% and 80/20% who show a homogeneous precipitate.

The curve of figure 2 highlights the evolution of the Ca/P atomic ratios during the formation of the hydroxyapatite in the absence and in the presence of chitosan. We can note that the first formed phases have Ca/P atomic ratios smaller compared to those quoted in the literature for hydroxyapatite precipitation in aqueous solution. At the beginning, the atomic ratios are very close to that of octocalcium phosphate ( $\text{Ca}_8(\text{HPO}_4)_2(\text{PO}_4)_4 \cdot 5\text{H}_2\text{O}$ , OCP: Ca/P=1,33). We can also note that the variation of the atomic ratios is faster for the first formed precipitates. Then these ratios increase gradually.

Both curves take the same form. However one can note a slightly slower evolution of the Ca/P atomic ratios in the case of the hydroxyapatite precipitation in the presence of chitosan. The phenomenon seems more accentuated at 360 minutes when the Ca/P atomic ratio is equal to the 1,59 in the case of composite, whereas it is 1,66 in the case of the formation of HAP without chitosan.

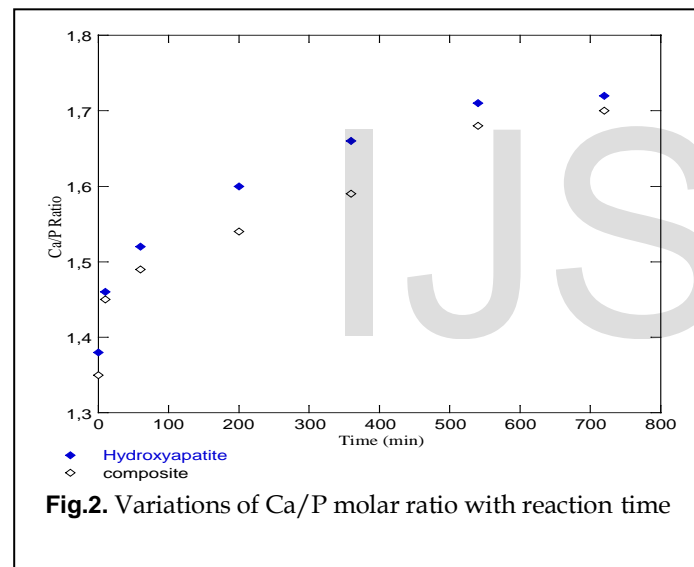


**Fig.2.** Variations of Ca/P molar ratio with reaction time

Figure 3 shows the FTIR spectra of the powder with Ca/P equal to 1,38 (a) and 1,66 (b) obtained in the absence of the chitosan and 1,59 (c) in the presence of chitosan. Spectrum (a) presents, in addition to the characteristic bands of the residues of synthesis ( $\text{H}_2\text{O}$ ,  $\text{CO}_3^{2-}$ ,  $\text{NO}_3^-$ ), bands 460, 550-600, 875, 960, 1020-1120  $\text{cm}^{-1}$  characteristics of the phosphates groups. The bands around 922  $\text{cm}^{-1}$  allotted to the vibration groups  $\text{HPO}_4^{2-}$  characteristic of triclinic octocalcium phosphate ( $\text{Ca}_8(\text{HPO}_4)_2(\text{PO}_4)_4 \cdot 5\text{H}_2\text{O}$ ) [22]. The spectrum (b) presents the same bands with the disappearance of the band at 922  $\text{cm}^{-1}$  and the appearance of the band with 630  $\text{cm}^{-1}$  allotted to grouping OH characteristic of the apatitic structure. The spectrum (c) of the bio-composite highlights a poorly crystallized apatitic structure where the band, located towards

630  $\text{cm}^{-1}$  characteristic of the grouping hydroxyl (OH), is not observed.

We can observe the bands characteristics of amide I groups but the bands characteristics of amid II and amino groups are not observed.

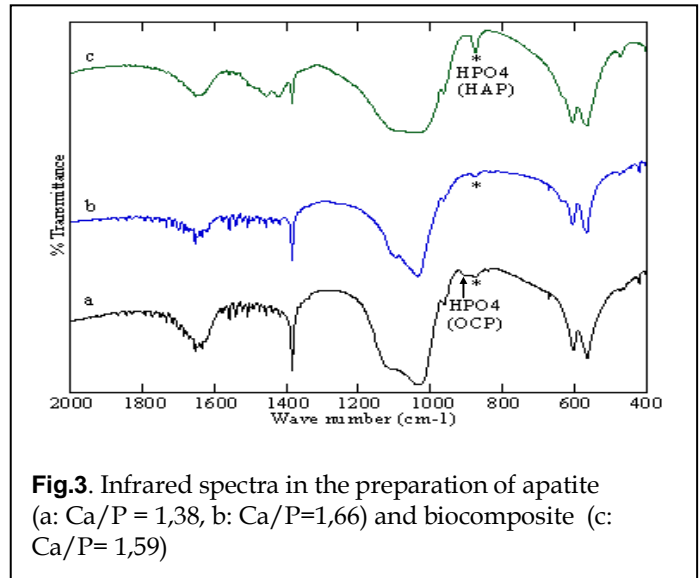


**Fig.3.** Infrared spectra in the preparation of apatite (a: Ca/P = 1,38, b: Ca/P=1,66) and biocomposite (c: Ca/P= 1,59)

Analyses by X-rays diffraction show in Figure 4a, for the compound with Ca/P=1,38, an amorphous structure. The first formed phase is indeed the octocalcium phosphate. According to the literature, the octocalcium phosphate is observed in various crystalline triclinic forms: apatitic or amorphous structure. Obtaining each one of these phases depends on the medium of the synthesis. The triclinic octocalcium phosphate has as a formula ( $\text{Ca}_8(\text{HPO}_4)_2(\text{PO}_4)_4 \cdot 5\text{H}_2\text{O}$ ) but the quantity of water associated with the structure is often variable [23],[24]. It is generally allowed that this compound could be present in the intermediate stages of the apatite bone mineral formation. It is thus proposed as a transitional state during the synthesis in aqueous solution of hydroxyapatite [25]. The diagram of X-ray diffraction of triclinic octocalcium phosphate is characterized by a peak (100) at the low angles towards  $2d=18,7\text{\AA}$  (25). The area of the small angles is difficult to examine, nevertheless one can notice the appearance of a peak with strong intensity towards  $2d=18,7\text{\AA}$ , allotted to the peak (100). X-ray diffraction patterns of the compound with atomic ratio 1,52 (figure 4(b)), highlights the disappearance of this peak and the evolution of the compound towards a poorly crystallized apatite.

Figure 5 illustrates FTIR spectra of the sample with Ca/P = 1,45 after the heat treatment at 900°C. Several bands at 725 and 1211  $\text{cm}^{-1}$  attributed to pyrophosphates were present and the bands at 630  $\text{cm}^{-1}$  assigned to OH were not observed. This agrees with the conversion of  $\text{Ca-HPO}_4$  into  $\beta\text{-CaP}_2\text{O}_7$  and with the dehydroxylation of apatitic tricalcium phosphate into  $\beta\text{-Ca}_3(\text{PO}_4)$ .

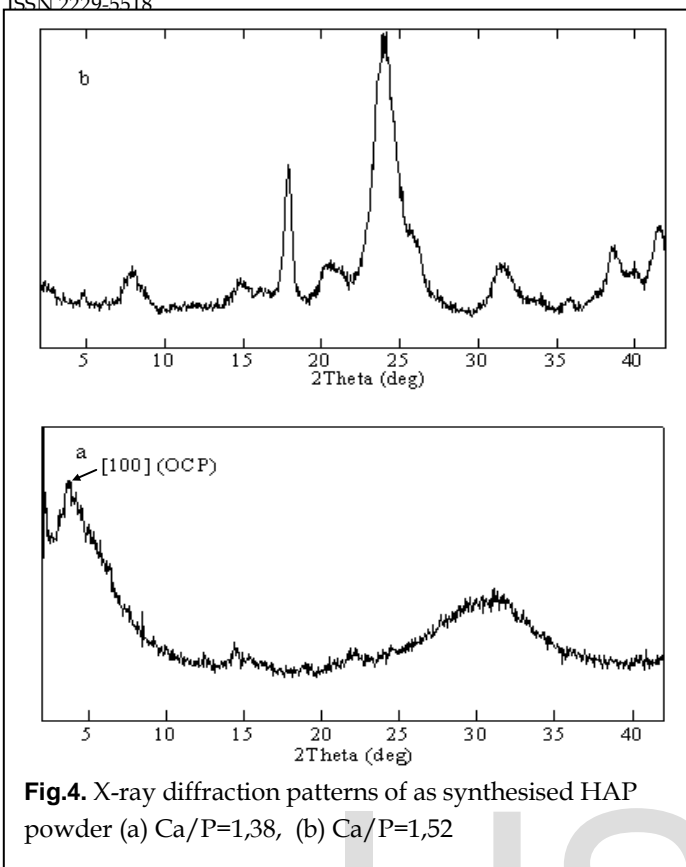


**Fig.4.** X-ray diffraction patterns of as synthesised HAP powder (a) Ca/P=1,38, (b) Ca/P=1,52



**Fig.5.** Infrared spectra in the preparation of powder with Ca/P= 1,45 calcined at 900°C

The sample with Ca/P=1,45 can be indicated by the following formula:  $Ca_{8,7}(HPO_4)_{0,3}(PO_4)_{4,7}(OH)$

During the maturation, the compound TCPap/chitosan, led at 360 min to the formation of a calcium-deficient apatite, which evolves then to hydroxyapatite. In the presence, as in

The physico-chemical properties of chitosan vary with the degree of deacetylation and the degree of polymerization [13],[14]. In our experiments; the chitosan is brought by the orthophosphoric acid solution at pH 1.8. It

the absence of the chitosan, the evolution towards hydroxyapatite took place at 540 to 720 min. The atomic ratio of final product (Ca / P =1,72) is slightly higher than the theoretical value (1,667) due to contamination of the sample by the air carbonates. The insertion of carbonate ions in the apatite structure turns at 900°C in lime trace (figure 6).

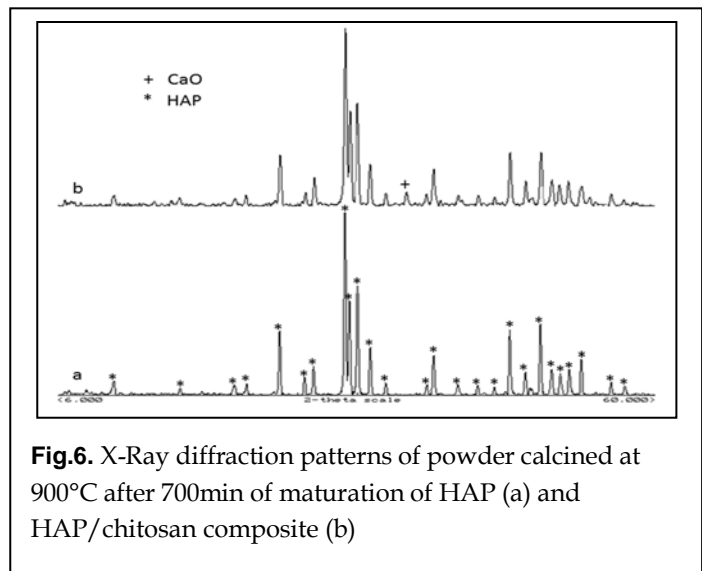
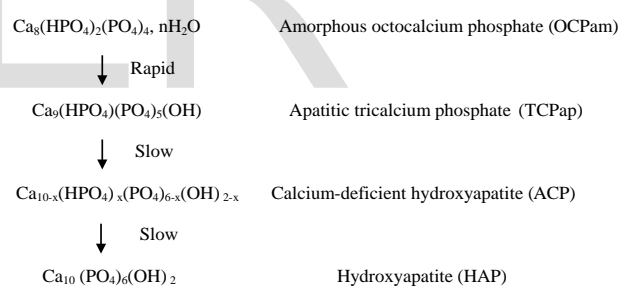


**Fig.6.** X-Ray diffraction patterns of powder calcined at 900°C after 700min of maturation of HAP (a) and HAP/chitosan composite (b)

We can conclude that the overall results show that the process of formation of the hydroxyapatite thus includes the following stages:



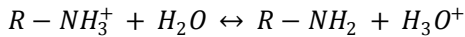
**Process of formation of intermediate states in the precipitation of hydroxyapatite**

Initially, we have the rapid formation of amorphous octocalcium phosphate (OCPam) thermodynamically unstable; it's transformed quickly into calcium phosphate with apatitic structure (TCPap). This compound then evolves to a calcium-deficient apatite, which is transformed gradually into hydroxyapatite. The same process is observed in the case of the preparation of the HAP in the presence of chitosan, but with a slight stabilization of the calcium-apatite structure.

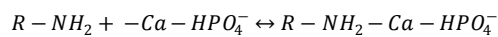
is thus positively charged; the intensity of this load is determined by the number of free functions amines, characterized by the degree of deacetylation:  $DD = 83 \pm 2\%$

in our case. The form  $NH_3^+$  allows the chitosan to be solubilized in the orthophosphoric acid solution.

Addition of the acid solution (orthophosphoric acid/chitosane) in the basic calcium solution (pH=10), leads to the chitosan precipitates according to the following balance of dissociation:



Thus, the form  $NH_2$  allows the precipitation of chitosan, following the establishment of high electrostatic hydrogen bond intermolecular and intramolecular and confers excellent chelating properties to it [26],[27]. In the basic-calcium solution, we have a simultaneous precipitation of chitosan and calcium phosphate compounds and the amino grouping chelated calcium according to the following:



The apatite structures (TCPa and ACP) contain many sites as  $HPO_4^-$  for the establishment of binding with the chitosan to form a stable  $RNH_2$ -apatite complex as  $RNH_2$ -TCPa and  $RNH_2$ -ACP (figure 7). This result shows the close association between chitosan and the hydrogenophosphate ( $Ca-HPO_4$ ) groups.

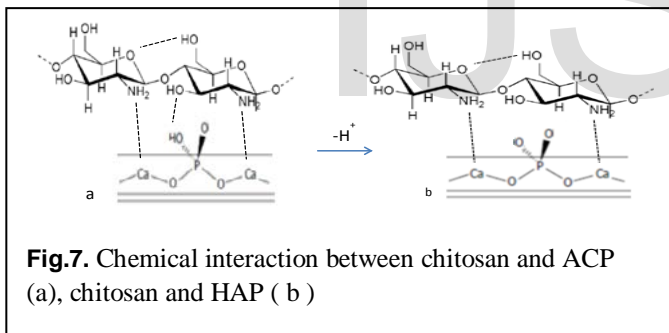


**Fig.7.** Chemical interaction between chitosan and ACP (a), chitosan and HAP ( b )

alkaline medium, the neutralization of  $HPO_4^-$  ( $RNH_2$ - $Ca-HPO_4^-$ ) ions favors the evolution to the hydroxyapatite crystals. It is important to note that when the pH is neutral or acidic, the system evolves to a Calcium-deficient apatite with rich  $HPO_4^-$  ion. This result is not described in this work. The study shows that Mw and DD of chitosan and pH of medium are the predominant parameters that can influence granular properties such as stoichiometry, homogeneity and agglomeration of bio-composite. The study also shows a possibility to obtain, in the same conditions, OCP/chitosan and TCP / chitosan bio-composites. The first product is obtained after 180min of maturation, while the second is obtained after 360 min of maturation. HAP / Chitosan composite are obtained after 720 min of maturation. These composites with varied molar

ratio Ca/P from 1,33 to 1,70 can have very interesting medical applications.

## 4 CONCLUSION

We have studied the mechanism of precipitation of hydroxyapatite in the presence and in the absence of chitosan. We have shown that the chitosan plays the role of a slight inhibitory in the formation of calcium-apatite by association between chitosan and the hydrogenous-phosphate groups. But the characteristics of the used chitosan (the degree of deacetylation and the molecular weight) and the alkali medium leads, after 720 min, to the formation of a material composed of hydroxyapatite associated with chitosan. The prepared composite can have very interesting medical applications for bone tissue engineering.

## REFERENCES

- [1] M. Bohner, Injury, Int. J. Care Injured 31 S4 (2000) S-D37-47.
- [2] S.V. Dorozhkin, biology and medicine, Materials 2 (2009) 399-498
- [3] Y. J. Yin, F. Zhao, X. F. Song, K. DeYao, W. Lu, , J. C. Leong, J. App. Polym. Sci. (2000) 77, 2929-2938.
- [4] B. C. Durucan, P. W. Brown, Advanced Engineering Materials. (2001) 3, 227-231.
- [5] M. Kikuchi, I T. koma, S. Itoh, H. Matsumoto, Y. Koyama, K. Takakuda, K. Shinomiya, J. Tanaka. Compos. Sci. Technol, (2004), 64, 819-825.
- [6] V. Jayachandrane Se-Kwon Kim. Drugs (2010) 8, 2252-2266
- [7] Guzman, R.; Nardecchia, S.; Gutierrez, M.C.; Ferrer, M.L.; Ramos, V.; del Monte, F.; Abarrategi, A.; López-Lacomba, J.L. *PLoS One* 2014, 9, e87149.
- [8] X. Liu, L. Ma, Z. Mao, Ch. Gaob, Adv Polym Sci (2011) 244: 81-128.
- [9] C. Xianmiao, L. Yubao,; Z. Yi, Z. Li, L. Jidong, W. Huanan, Mater. Sci.Eng. C (2009) 29, 29-35.
- [10] H. Li, Ch. Zhou, M. Zhu, J. Tian, J. Rong, Journal of Biomaterials and Nanobiotechnology, (2010) 1, 42-49.
- [11] Luciano Pighinelli, Magdalena Kucharska. Journal of Biomaterials and Nanobiotechnology, 2014, 5, 128-138.
- [12] Luciano Pighinelli, Magdalena Kucharska, Journal of Biomaterials and Nanobiotechnology, 2013, 4, 20-29
- [13] A. Domard. Carbohydr.Polym, (2010) 04, 083.
- [14] Jolanta Kumirska, Mirko X. Weinhold, Małgorzata Czerwicka, Biomedical Engineering, Trends in Materials Science, (2011) ISBN: 978-953-307-513-6.
- [15] S.-J. Ding, Dental Materials Journal, Vol. 25, No. 4, (2006) 706-712.
- [16] S. Viala, M. Frenche, J.L. Lacout, Annales de Chimie Science des Matériaux, (1998) 23, 69-72
- [17] M. D. Weir H.K. Xu, J Biomed Mater Res A, (2010) 94(1): 223-233.
- [18] Leroux, L.; Hatim, Z.; Frèche, M.; Lacout, J. L. Bone, (1999) 25(2 Suppl), 31S-34 S.
- [19] J.L. Lacout. Z. Hatim, M. Freche, (2003) Patent 9803459.
- [20] R. Z. LeGeros, M. H. Taheri, G. M Quirlogico, J. P. LeGeros. Proc. 2nd International Congress on Phosphorous Compounds Boston, (1980) 89-103.
- [21] R. Z. LeGeros. In: Tooth Enamel IV, Reearnhead RW, Suga S

- (Eds). Elsevier: Amsterdam, (1984) 2, 32-36.
- [22] M. Mathew, W. E. Brown, L.W. Schroeder, B. Dickens. J. Cryst. Spectrosc. Res. (1988) 18, 235-250.
- [23] J. Elliott. New York. Elsevier, (1994).
- [24] W. E. Brown, M. Matthew, M. S. Tung. Prog. Crystal. Growth. Charact, (1981) 4, 59-87.
- [25] W. E. Brown, L. C. Chow. In: Brown PW, editor. Westerville, OH: Cem Res Prog American Ceramic Society, (1986) 351-79.
- [26] K. Inoue, Y. Baba, K. Yoshisuka. Bull. Chem. Soc. Jpn. (1993) 66, 2915-2921.
- [27] R. Maruca, B. J. Suder, J. P. Wightman. J. Appl. Polym. Sci, (1982) 27, 4827-4837.

IJSER